*Proc. Natl. Acad. Sci. USA*
Vol. 86, pp. 4087–4091, June 1989
Biophysics

# Single-molecule fluorescence detection: Autocorrelation criterion and experimental realization with phycoerythrin

(laser-induced fluorescence/femtomolar sensitivity/fluorescence assays/phycoerythrin oligomers)

KONAN PECK*, LUBERT STRYER†, ALEXANDER N. GLAZER‡, AND RICHARD A. MATHIES*

*Department of Chemistry, University of California, Berkeley, CA 94720; †Department of Cell Biology, Stanford University School of Medicine, Stanford, CA 94305; and ‡Department of Microbiology and Immunology, University of California, Berkeley, CA 94720

*Contributed by Lubert Stryer, February 10, 1989*

ABSTRACT **A theory for single-molecule fluorescence detection is developed and then used to analyze data from subpicomolar solutions of B-phycoerythrin (PE). The distribution of detected counts is the convolution of a Poissonian continuous background with bursts arising from the passage of individual fluorophores through the focused laser beam. The autocorrelation function reveals single-molecule events and provides a criterion for optimizing experimental parameters. The transit time of fluorescent molecules through the 120-fl imaged volume was 800 μs. The optimal laser power (32 mW at 514.5 nm) gave an incident intensity of $1.8 \times 10^{23}$ photons·cm$^{-2}$·s$^{-1}$, corresponding to a mean time of 1.1 ns between absorptions. The mean incremental count rate was 1.5 per 100 μs for PE monomers and 3.0 for PE dimers above a background count rate of 1.0. The distribution of counts and the autocorrelation function for 200 fM monomer and 100 fM dimer demonstrate that single-molecule detection was achieved. At this concentration, the mean occupancy was 0.014 monomer molecules in the probed volume. A hard-wired version of this detection system was used to measure the concentration of PE down to 1 fM. This single-molecule counter is 3 orders of magnitude more sensitive than conventional fluorescence detection systems.**

Fluorescence spectroscopy is an ideal method for quantitating the concentration and location of fluorescent molecules because of its high sensitivity. Fluorescence detection is widely used in immunoassay, flow cytometry, and chromatographic analysis, where the detection limits are from $10^3$ to $10^6$ fluorescent molecules (1, 2), and in automated DNA sequence analysis, where the detection limits are $10^6$–$10^7$ molecules (3, 4). The development of more sensitive fluorescence detection systems is important because it would permit new applications of this technique in analytical chemistry, biology, and medicine.

In the quest for enhanced sensitivity, Hirschfeld (5) used evanescent-wave excitation to detect an antibody molecule labeled with 80 fluorescein molecules adsorbed on a glass slide. Using a flowing sample, Dovichi *et al.* (6) achieved a detection limit of 22,000 rhodamine 6G molecules in a 1-s integration time, and Nguyen *et al.* (7) extended this limit to 800 molecules with hydrodynamically focused flows. Mathies and Stryer (8) pointed out the limits imposed by photodestruction and detected three molecules of B-phycoerythrin (PE) in a probe volume of 10 pL. PE is an attractive fluorophore for enhancing sensitivity because of its high absorption coefficient, near unity fluorescence quantum yield, and large emission Stokes shift (9–11). Recently, Nguyen *et al.* (12) observed bursts of fluorescence when a 1 pM solution of PE was flowed through a focused laser beam, and they interpreted these bursts as being due to the passage of individual molecules. In this paper, we present a theory for single-molecule fluorescence detection and apply it in detecting phycoerythrin at concentrations as low as 1 fM.

The publication costs of this article were defrayed in part by page charge payment. This article must therefore be hereby marked "*advertisement*" in accordance with 18 U.S.C. §1734 solely to indicate this fact.

## THEORY

Consider a solution of fluorophores flowing through a focused laser beam. The emission from the illuminated volume consists of bursts of fluorescence from molecules passing through the beam superimposed on a continuous background due to Rayleigh and Raman scattering from the solvent (Fig. 1*A*). The mean rate $k_b$ (photons·s$^{-1}$) of background scattering by the solvent is

$$k_b = \sigma_b I, \quad [1]$$

and the mean rate $k_f$ (photons·s$^{-1}$) of fluorescence emission by a molecule in the beam assuming nonsaturating excitation conditions is

$$k_f = \sigma_a I Q = 3.8 \times 10^{-21}\, \varepsilon Q \mathbf{P}/(\pi\omega^2). \quad [2]$$

Here $I$ is the light intensity (photons·cm$^{-2}$·s$^{-1}$), $\sigma_b$ is the sum of the Rayleigh and Raman scattering cross sections of the solvent, $\sigma_a$ is the absorption cross section of the fluorescent molecule, $Q$ is the quantum yield of fluorescence, $\varepsilon$ is the extinction coefficient, $\omega$ is the beam $1/e^2$ radius, and $\mathbf{P}$ is the laser power (photons·s$^{-1}$). Fluorescence emission by a molecule is ultimately terminated by photodestruction (8, 13). The rate of photodestruction $k_d$ (s$^{-1}$) is

$$k_d = \sigma_a I \Phi, \quad [3]$$

where $\Phi$ is the quantum yield of photodestruction. The mean lifetime $t_d$ of a fluorescent molecule in the beam is $1/k_d$.

The number of detected counts $n_s$ in a time interval $\Delta t$ is the sum of $n_b$, the counts from solvent scattering, and $n_f$, the counts from fluorescence emission. The mean number of background counts $\mu_b$ is given by

$$\mu_b = k_b \Delta t E_b, \quad [4]$$

where $E_b$ is the collection efficiency from solvent scattering. The probability $P_b$ of having $j$ counts of background scattering in a time interval $\Delta t$ is given by the Poisson distribution:

$$P_b(j) = \frac{\mu_b^j e^{-\mu_b}}{j!}. \quad [5]$$

Likewise, the mean number of fluorescence counts $\mu_f$ arising from a molecule in the beam is given by

$$\mu_f = k_f \Delta t E_f. \quad [6]$$

Abbreviation: PE, B-phycoerythrin.

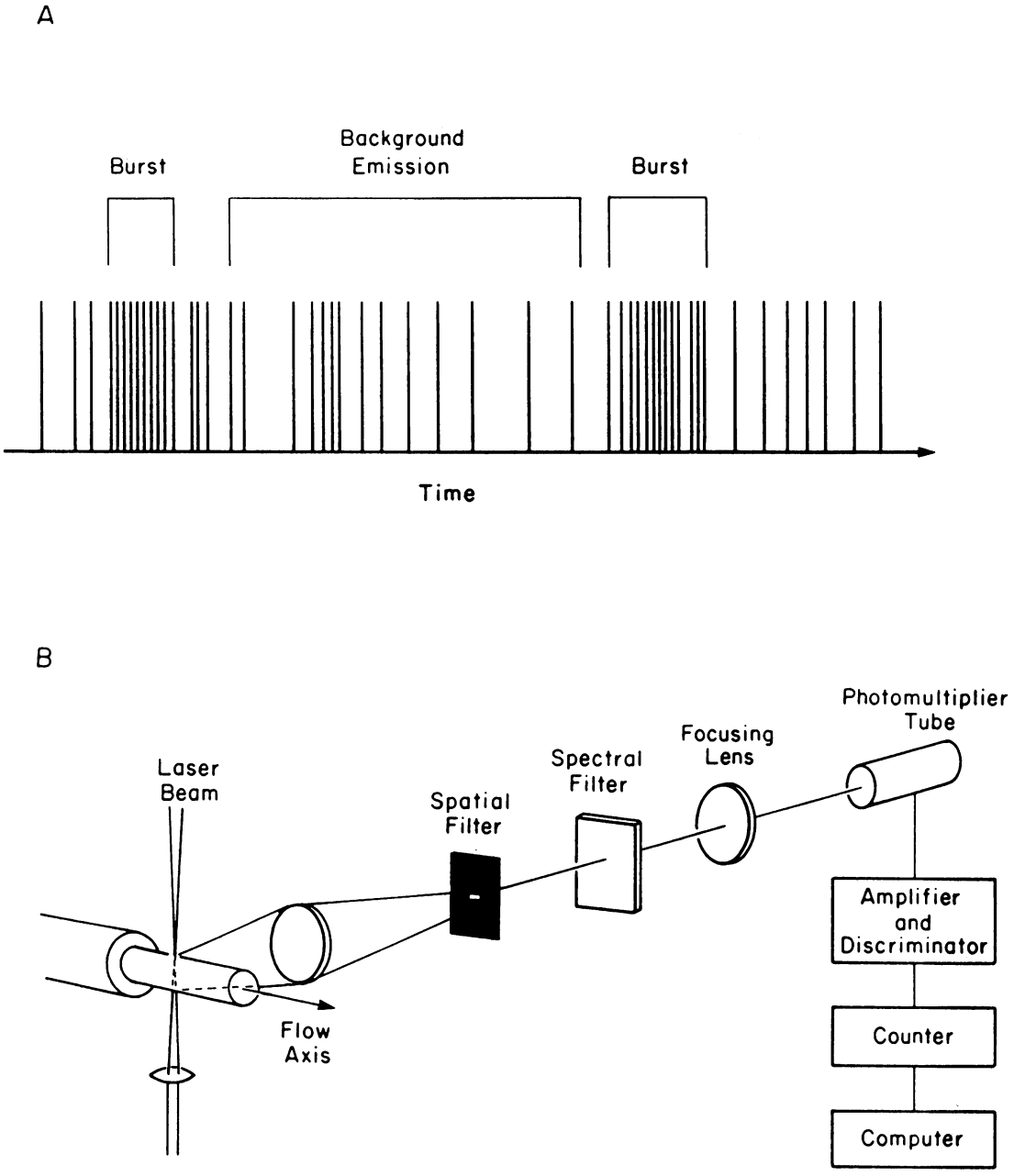


FIG. 1. (*A*) Illustration of the concept of single-molecule fluorescence detection. When a fluorescent molecule flows through a laser beam, a burst of photons is generated; single-molecule events can be distinguished from the Poisson-distributed background if the fluorescence emission rate is higher than the background emission rate. (*B*) Experimental apparatus for single-molecule fluorescence detection. The 514.5-nm output from an argon-ion laser is focused to a 8-$\mu$m-diameter spot in a capillary tube through which a sample solution is flowed. The resulting fluorescence is collected at 90° and passed through spatial and spectral filters to the detection system.

When a molecule is in the beam, the probability $P_f$ of having $j$ counts of fluorescence emission is

$$P_f(j) = \frac{\mu_f^j e^{-\mu_f}}{j!}. \quad [7]$$

When there is no fluorescent molecule in the beam, $P_f(0) = 1$.

Fluorescence from single molecules in the beam and scattering from solvent are two independent processes. In a given time interval, the observed counts can come from any possible combination of scattering and fluorescence. The probability $P_s(m, \Delta t)$ of observing $m$ counts in a time interval $\Delta t$ is given by

$$P_s(m, \Delta t) = \sum_j P_b(j,\Delta t)\, P_w(m - j,\Delta t). \quad [8]$$

In other words, the observed distribution of counts is the convolution of background scattering ($P_b$) and fluorescence emission ($P_w$) occurring in an observation window of duration $\Delta t$. $P_w$ is a modified fluorescence probability function that takes into account all possible temporal arrangements of the fluorescent molecule with respect to the observation window.

Single molecule detection is optimized by maximizing the ratio of $n_f$ (the signal) to $(n_b)^{1/2}$ (the mean fluctuation in the background). As the light intensity increases, $n_f$ increases linearly until it reaches a maximal asymptotic value when the absorption rate equals the maximum emission rate. The background $n_b$ simply increases linearly with light intensity. Thus, there should be a power at which the experiment is optimized. The most favorable illumination intensity can be experimentally determined by monitoring the

autocorrelation of $n_s$. The autocorrelation parameter $R_s(\tau)$ is defined as

$$R_s(\tau) = \sum_j n_s(j)n_s(j+\tau) = R_b(\tau) + R_f(\tau) + R_{bf}(\tau). \quad [9]$$

$R_s$ is the sum of the autocorrelation of $n_b$, the autocorrelation of $n_f$, and the crosscorrelation of $n_b$ and $n_f$. These contributions to $R_s$ are given by

$$R_b(\tau) = \sum_j n_b(j)n_b(j+\tau), \quad [10]$$

$$R_f(\tau) = \sum_j n_f(j)n_f(j+\tau), \quad [11]$$

$$R_{bf}(\tau) = 2\sum_j n_f(j)n_b(j+\tau). \quad [12]$$

For $\tau > 0$, $R_b$ and $R_{bf}$ are independent of time because background scattering is a continuous process with Poisson-distributed probability of occurrence. In contrast, since the fluorescence emission from an individual molecule in the beam is temporally correlated, only $R_f(\tau)$ has appreciable magnitude and temporal decay for values of $\tau > 0$. The decay of $R_f$ will be determined by the photodestruction time ($t_d$) or by the transit time of the molecule through the beam ($t_m$), whichever is shorter.

It is useful to define a parameter $M$ as

$$M = \frac{R(1) - R(\infty)}{[R(\infty)]^{1/2}}, \quad [13]$$

where $R(1)$ and $R(\infty)$ are the values of $R$ at times short and long, respectively, compared with $t_m$ and $t_d$. Because $R_b(1) = R_b(\infty)$ and $R_{bf}(1) = R_{bf}(\infty)$, $R(1) - R(\infty)$ is proportional to $n_f^2$. Also, if the sample is very dilute, $R(\infty) \approx n_b^2$. Hence $M$ is nearly proportional to $n_f^2/n_b$ and therefore can be used as a figure of merit to set the illumination intensity. The correlation analysis presented here is formally similar to that used in scanning fluorescence correlation spectroscopy (14, 15). However, fluorescence correlation spectroscopy is typically performed with $\approx 10^3$ molecules in the illuminated volume.

## MATERIALS AND METHODS

The experimental setup is depicted in Fig. 1*B*. The stabilized (0.5%) 514.5-nm beam from a Spectra-Physics 2020 argon-ion laser was focused by a 32-mm focal length microscope objective to a 4-$\mu$m radius at the center of a flowing sample stream contained in a 0.5 mm × 0.5 mm square capillary tube. The flow velocity was chosen to be 1 cm/s so that the transit time of molecules through the laser beam was 800 $\mu$s. The laser polarization was oriented in the scattering plane to minimize Rayleigh and Raman scattering from water. Fluorescence emission was collected by a ×40, 0.65-NA (numerical aperture) microscope objective and imaged onto a 100 $\mu$m × 400 $\mu$m slit. This spatial filter defined a probe volume of 0.12 pl (8-$\mu$m diameter × 2.5 $\mu$m) and rejected scattering and fluorescence from capillary walls. A 575-nm fluorescence interference filter with a 40-nm band pass (Omega Optics, Brattleboro, VT) was used to reject Rayleigh and Raman scattering. The fluorescence was detected with an RCA 31034A photomultiplier tube and a PAR 1120 amplifier/discriminator.

To produce the pulse-height distributions and autocorrelations, photoelectron pulses were counted by a fast counter/timer (50-$\mu$s gate time) interfaced to an IBM PC/AT computer. For the autocorrelation analysis, data were processed as collected. For the pulse-height analysis, data were grouped in 100-$\mu$s bins.

In the low-concentration experiments, we used a hard-wired single-molecule gating circuit, where pulses from the amplifier/discriminator were passed to an analog moving-sum circuit followed by a discriminator. The moving-sum had a response time of 280 $\mu$s, and the discriminator threshold was referenced to the mean count rate (10 ms average) to correct for drift in the background count rate. Each sample was counted for 1000 s.

**Preparation of PE Oligomers.** To 0.55 ml (3.5 mg; 25.6 $\mu$M) of *Porphyridium cruentum* PE (16) in 0.1 M sodium phosphate/0.1 M NaCl, pH 7.40, was added 10 $\mu$l of freshly-prepared 15 mM 3-(2-pyridyldithio)propionic acid *N*-hydroxysuccinimide ester solution in methanol. After 70 min at 23°C, half of the reaction mixture was passed through a Sephadex G-25 (bead size, 20–80 $\mu$m) column (0.75 × 15 cm) to separate the protein derivative from excess reagent. To the other half of the reaction mixture, 10 $\mu$l of 1 M dithiothreitol in the pH 7.40 buffer was added, and the mixture was allowed to stand at 23°C for 45 min. The thiolated-PE derivative was separated from small molecules by gel filtration as described above. The thiolated-PE and the 3-(2-pyridyldithio)propionyl derivative of PE were mixed in a molar ratio of 0.8:1.0 and allowed to react at 23°C for 19 hr. The reaction mixture was then layered on linear 0.25-1.5 M sucrose density gradients in the pH 7.40 buffer and spun in a Sorvall TST 41.14 rotor at 118,400 × $g_{avg}$ for 20 hr at 15°C. Five well-resolved bands were seen on the gradient in the relative proportions monomer < dimer > trimer >> tetramer >> pentamer.

The concentration of $\approx$0.1 $\mu$M stock solutions of PE monomer and dimer were determined spectrophotometrically based on an absorption coefficient of 2.4 × $10^6$ $cm^{-1}\cdot M^{-1}$ at 545 nm (16). The solutions were serially diluted to various concentrations in unbuffered (pH 6–7) 50 mM sodium chloride solution just before use. All solutions were centrifuged at 13,000 rpm (27,500 × $g_{avg}$) for 15 min and degassed to eliminate scattering particles and air bubbles. Solutions were stored in polypropylene flasks, and the entire flow system was made of plastic to minimize protein adsorption. To remove adsorbed protein, the flow system was flushed with detergent (RBS 35, Pierce) and nitric acid.

**Distribution Simulations.** In the simulation of $n_s$, the time interval between successive points is chosen to be small compared with $t_m$ and $t_d$. For $z$ molecules passing through the beam per second, the probability $P_a$ that a molecule has entered the beam in an interval $\Delta t$ is $z\Delta t$. It is assumed that the concentration is sufficiently low that (*i*) $z^{-1} >> t_m$ and (*ii*) no more than one fluorescent molecule is present in the illuminated volume at any time. A random number $r_1$, distributed between 0 and 1, is used with Eq. **5** to determine $n_b$. Two additional random numbers $r_2$ and $r_3$ determine whether the fluorescent molecule is present in the beam and still emitting. A molecule has entered the beam if $r_2 \le P_a$. It stays in the beam for an interval $t_m$ and is emitting at time $t$ after entering if $r_3 \le e^{-t/t_d}$. If so, another random number $r_4$ determines $n_f$ according to Eq. **7**. Otherwise, $n_f = 0$.

## RESULTS AND DISCUSSION

The challenge in single-molecule detection is to find conditions that make the single-molecule events as bright as possible compared with the fluctuations in the background count rate. The laser is tightly focused to lower the probability of multiple molecules in the probe volume and to improve the fluorescence-to-background ratio. The transit time should be somewhat less than the photodestruction time so that photodestruction does not complicate the autocorrelation analysis.[§] Once these parameters are set, the only

[§]The measured photodestruction time for PE under the experimental conditions used here was always ≥1 ms. This time is longer than that calculated according to Eq. **3** for a photodestruction quantum yield of 1 × $10^{-5}$ because of ground-state depletion at high light intensities.

variable is the total laser power. The goal is to maximize the emission rate $k_f$ compared with noise in the background, which is proportional to $(k_b)^{1/2}$. These numbers can be directly measured by autocorrelation analysis.

Experimentally observed and simulated autocorrelation traces of PE dimers with laser powers from 13 mW to 38 mW are shown in Fig. 2. Since the random Poisson background gives a flat autocorrelation except for the noise spike at $R(0)$, it is evident from the shoulder in the experimental traces at short times that we are seeing correlated bursts of fluorescence. $R_f$ in the autocorrelation traces approaches $R_s(\infty)$ at approximately the transit time (800 $\mu$s), as predicted. This clearly shows that we are seeing clustered emission events with a duration of about $t_m$. The excellent agreement between the experimental and simulated data for realistic parameters indicates further that we are seeing single-molecule events. Since $R(0)$ contains the noise $\delta$ function, the data are best discussed in terms of $R_f(1)$ where $R_f(1) = R_s(1) - R_s(\infty)$. $R_f(1)$ grows with power from 13 mW to 32 mW but does not increase at powers above 32 mW. Thus, when the power is greater than 32 mW, $k_f$ has attained its maximum emission rate. Powers higher than 32 mW do not increase the burst amplitude, but they do increase the background emission rate and the concomitant background fluctuations.

To find the optimal laser power, the figure of merit $M$ is plotted versus laser power in Fig. 3. Since $M$ is proportional to the square of the signal-to-noise ratio, it provides a criterion for choosing the optimal laser power. The optimum is 32 mW, which corresponds to a focused light intensity of $1.8 \times 10^{23}$ photons·cm$^{-2}$·s$^{-1}$ and a mean time between absorptions of 1.1 ns. The flatter experimental curve compared with the simulated data (dotted) may arise because of background fluorescence emission from molecules just outside the probed volume or from impurities in the sodium chloride solution.

The distribution and autocorrelation functions for blank, PE monomers, and PE dimers are presented in Fig. 4. The blank closely follows a Poisson distribution with a mean value of 0.98 per 100 $\mu$s, and the autocorrelation shows random noise at all times. The distribution function for PE monomer shows marked deviation from a Poisson distribution: there are a significant number of occurrences of up to 11

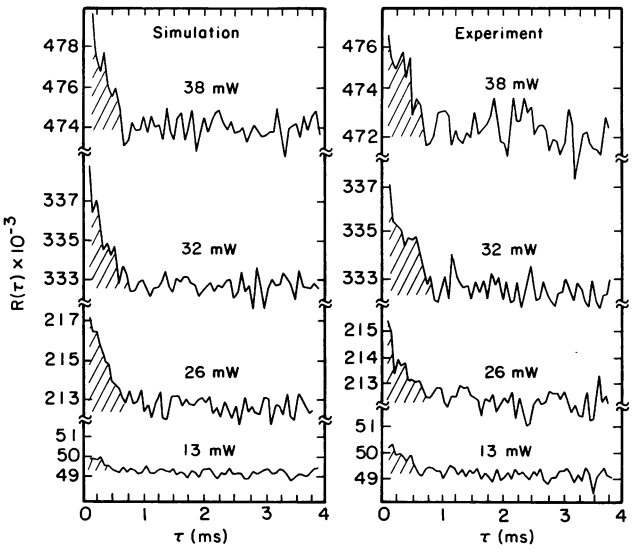


FIG. 2. Experimental and simulated autocorrelation traces for 100 fM PE dimers at the indicated laser powers. Each bin is 50 $\mu$s, and the number of data points in each autocorrelation analysis is $1.12 \times 10^6$. In the simulations, $k_b$ was 0.42, 0.86, 1.0, and 1.3 counts per 100 $\mu$s and $k_f$ was 1.2, 2.4, 2.8, and 2.8 counts per 100 $\mu$s for laser powers of 13, 26, 32, and 38 mW, respectively.

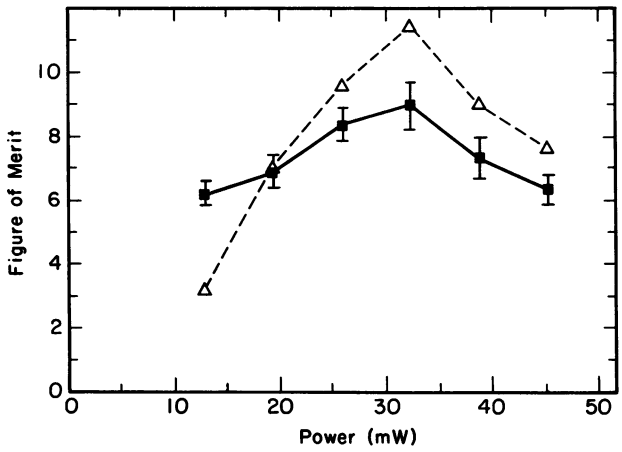


FIG. 3. Plot of the figure of merit $M$ versus laser power based on the data in Fig. 2. Experimental data (——) and simulated data (---) are shown.

counts per 100 $\mu$s. The Poisson curve $P_b$ is shifted to slightly higher values and acquires a long tail by convolution with $P_f$. The fluorescence hump in the distribution plot for the dimer is more obvious, and it extends to higher count rates. The autocorrelation traces also show the presence of clustered events of duration ≈800 $\mu$s. If we are indeed seeing single-molecule events, then the emission rate $k_f$ should be twice as large for the dimer. $R_f(1)$ depends linearly on the concentration and quadratically on $k_f$. Hence, the dimer at half the concentration of the monomer should exhibit $R_f(1)$ that is twice as large. This is in fact seen in Fig. 4, again demonstrating that we are observing single-molecule events. By modeling the autocorrelation traces in Fig. 4, we determined that the mean emission rate of monomers is 1.5 counts per 100 $\mu$s and that of dimers is 3.0 counts per 100 $\mu$s. This gives 12 counts for a monomer burst and 24 counts for a dimer burst, which are well above the 8 count per 800-$\mu$s background.

To explore the detection limits of single-molecule counting, PE monomers and dimers from 1 fM to 1 pM were examined with the hard-wired single-molecule gating circuit. Because the distribution of the observed count rate is the convolution of background scattering and fluorescence emis-

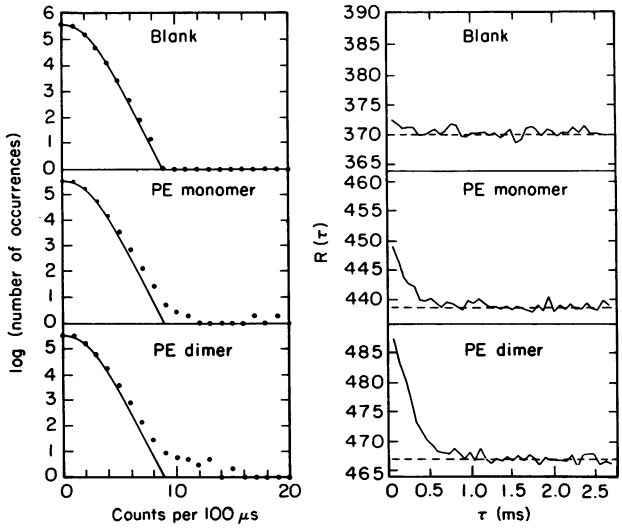


FIG. 4. Comparison of burst-distribution (*Left*) and autocorrelation traces (*Right*) for blank (50 mM NaCl), PE monomer (0.2 pM), and PE dimer (0.1 pM). The solid lines are calculated Poisson distribution curves with a mean count rate of 0.98 per 100 $\mu$s. The number of data points in each analysis is $1.68 \times 10^6$.

sion, any discriminator setting will necessarily report both real single-molecule and false background events, unless the fluorescence emission rate is much greater than $k_b$. Fig. 5 presents the log of the number of single-molecule events versus the log of the concentration. The regression lines of these two plots have a slope fairly close to 1, 1.05 for the monomer data, and 1.15 for dimer data. The linear concentration dependence strongly supports the idea that we are seeing *single*-molecule events. The dynamic range is limited by sampling time at low concentrations and by multiple occupancy at high concentrations. At concentrations greater than 1 pM, the mean of the Poisson curve will shift up because of the fluorescence from multiple molecules in and around the probe volume.

To detect single-molecule bursts, one must ensure that the probability of observing emission from two molecules simultaneously in the beam is negligible. In the distribution function, the probability of detecting zero counts from the fluorescent sample should differ from that of the solvent by less than 10%. A convenient test is that the mean number of counts in the sample should increase by less than 10% compared with the blank, as observed here. In the experiments of Nguyen *et al.* (12), performed with 1 pM PE, the most probable count rate with PE is double that in the blank and their probability for single occupancy (0.34) gives a double-occupancy probability of 0.11. It seems likely that most of their fluorescence bursts were due to the simultaneous presence of two or more molecules in the imaged volume.

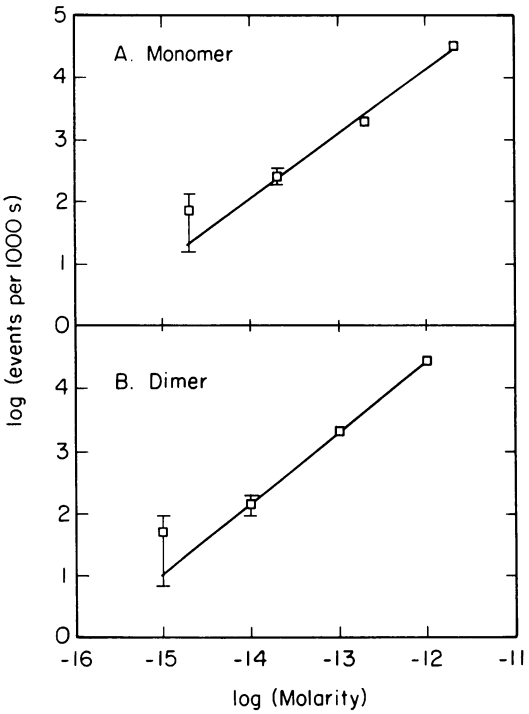


FIG. 5. Fluorescence detection limits with single-molecule counting. (*A*) PE monomer with concentrations from 2 fM to 2 pM. (*B*) PE dimer with concentrations from 1 fM to 1 pM. To reduce the number of false events, the discriminator threshold was set quite high so that only ≈15% of the actual monomer events and 20% of the dimer events were detected. This gave 3000 background events in 1000 s for the monomer experiments and 1700 for the dimer experiments. After background subtraction, the number of monomer events was 70, 270, 2060, and 34,600 and the number of dimer events was 50, 140, 2140, and 27,800.

In conclusion, we have identified key parameters in single-molecule fluorescence detection and developed criteria for optimizing single-molecule counting. The distribution plots for PE monomers and dimers show that high emission rate non-Poisson events are occurring. The autocorrelation analysis shows that these are true molecule events with the correct duration. This is reinforced by the finding that PE dimers give twice the mean burst height observed for monomers and the same burst duration. The autocorrelation analysis also makes possible the adjustment of the incident laser power to optimize the emission rate from the molecules while keeping background fluctuations to a minimum. A hard-wired analog single-molecule detection system is then used to explore the low-concentration limits of single-molecule detection. We can detect PE monomers and dimers at concentrations as low as 1 fM. This is a 1000-fold improvement over previous sensitivity limits (8). The enhanced sensitivity afforded by single-molecule detection should be directly applicable to the detection of fluorescent molecules or fluorescently labeled peptides in HPLC or capillary electrophoresis (17). The concepts presented here should also be very useful in optimizing fluorescence detectors in flow cytometry and in DNA sequencing.

We thank Dr. Denis Baylor for helpful comments on the autocorrelation analysis. This research was supported by grants from the National Science Foundation (DIR 87-20382 and DMB 88-16727), by a grant from the National Institutes of Health (GM 24032), and by the Director, Office of Energy Research, Office of Health and Environmental Research, Physical and Technological Research Division, of the U.S. Department of Energy under Contract DE-FG03-88ER60706.

1. Milby, K. H. & Zare, R. N. (1984) *Am. Clin. Prod. Rev.* **3,** 14–19.
2. Muirhead, K. A., Horan, P. K. & Poste, G. (1985) *Bio/Technology* **3,** 337–356.
3. Ansorge, W., Rosenthal, A., Sproat, B., Schwager, C., Stegemann, J. & Voss, H. (1988) *Nucleic Acids Res.* **16,** 2203–2207.
4. Smith, L. M., Sanders, J. Z., Kaiser, R. I., Hughes, P., Dodd, C., Connell, C. R., Heiner, C., Kent, S. & Hood, L. E. (1986) *Nature (London)* **321,** 674–679.
5. Hirschfeld, T. (1976) *Appl. Opt.* **15,** 2965–2966.
6. Dovichi, N. J., Martin, J. C., Jett, J. H., Trkula, M. & Keller, R. A. (1984) *Anal. Chem.* **56,** 348–354.
7. Nguyen, D. C., Keller, R. A. & Trkula, M. (1987) *J. Opt. Soc. Am.* **4,** 138–143.
8. Mathies, R. A. & Stryer, L. (1986) in *Fluorescence in the Biological Sciences*, eds. Taylor, D. L., Waggoner, A. S., Lanni, F., Murphy, R. F. & Birge, R. (Liss, New York), pp. 129–140.
9. Oi, V. T., Glazer, A. N. & Stryer, L. (1982) *J. Cell Biol.* **93,** 981–986.
10. Glazer, A. N. & Stryer, L. (1984) *Trends Biochem. Sci.* **10,** 423–427.
11. Kronick, M. N. (1986) *J. Immunol. Methods* **92,** 1–13.
12. Nguyen, D. C., Keller, R. A., Jett, J. H. & Martin, J. C. (1987) *Anal. Chem.* **59,** 2158–2161.
13. Hirschfeld, T. (1976) *Appl. Opt.* **15,** 3135–3139.
14. Meyer, T. & Schindler, H. (1988) *Biophys. J.* **54,** 983–993.
15. Petersen, N. O. (1986) *Biophys. J.* **49,** 809–815.
16. Glazer, A. N. & Hixson, C. S. (1977) *J. Biol. Chem.* **252,** 32–42.
17. Cheng, Y. F. & Dovichi, N. J. (1988) *Science* **242,** 562–564.